Mechanical Characteristics and Correlation Analysis of Crack Propagation and Slip Cracking in Asphalt Pavement Surface Layer

Yin Zhenyu

School of Civil and Transportation Engineering, Henan University of Urban Construction, Pingdingshan Henan 467041, China
E-mail: 30070101@hncj.edu.cn

Abstract

With the rapid development in the field of road traffic, the problems of slip cracking and U-shaped cracks on the surface of asphalt pavement are becoming more and more prominent, which seriously affect the safety and service life of roads. In order to solve this problem, a reliable asphalt pavement model is established in this study by combining the joint simulation and secondary development of experimental test parameters. The model can accurately simulate the slip cracking of asphalt pavements under different conditions and provide detailed parametric analysis of the factors affecting crack development. The results show that the inter-ply bond damage no longer deteriorates when the inter-ply strength is 0.3 MPa, indicating that the form of inter-ply contact plays a role in controlling the development of slip cracks. In addition, the maximum interlayer shear stress increased by 21.1% during the increase of vehicle axle load from 100 kN to 200 kN on the asphalt pavement, which led to an increase in the length of slip cracks. Meanwhile,

the maximum longitudinal tensile stress in the asphalt pavement surface layer increased by 10.2% and the maximum shear stress increased by 18.3% when the elastic modulus of the asphalt pavement surface layer was increased from 7500 MPa to 14500 MPa.

1 Introduction

The rapid development in the field of transportation has marked entry into a new era based on the construction of high-grade highways such as expressways and primary roads. At present, highways have become an important transportation facility supporting the economic development of countries around the world. By the end of 2020, the total mileage of highways in China has reached 16.1 million kilometers and is in first place in the world [1]. In the construction of highways around China, asphalt pavement is widely used for its advantages such as good surface levelness, no seepage joints, low vibration, low noise, comfortable driving, and can be built in stages [2, 3] Nowadays, more than 80% of highways in China use asphalt pavement [4] With the popularity of asphalt pavement, the research and management of asphalt pavement diseases are very important. Slip cracks are common in asphalt pavement soon after construction, especially at longitudinal slopes, road intersections, parking points, etc [5]. Slip cracks are commonly found in asphalt pavements shortly after construction, especially at long longitudinal slopes, road intersections, and parking lots. Slip cracks are usually caused by the poor bonding between the top layer and the middle layer of the asphalt pavement and the huge horizontal force on the top layer which cannot be transferred to the bottom layer well, thus leaving the top layer to bear alone and causing the surface to be pulled and cracked [6]. The surface is cracked and damaged. Therefore, in some road sections with high traffic flow, the load generated by vehicles varies greatly and has a large impact on the pavement structure, which can easily cause damage to the pavement structure function [7]. In longitudinal slope road sections, the frequent acceleration of vehicles when climbing and frequent braking when going downhill, especially large load vehicles, will make the pavement produce a large longitudinal shear force in the longitudinal direction of traffic. When the shear resistance between layers of asphalt pavement is poor, it is very easy to cause longitudinal slip cracks. Yared H et al. [8] studied the effect of

two-wheel axle loading on the generation of surface cracking and fatigue life of pavement surface by establishing a finite element asphalt pavement model based on fracture mechanics, the ad also concluded that a thicker surface layer would reduce the probability of surface cracking. Emery [9] proposed that in addition to tensile and shear stresses, surface cracks in asphalt pavements are also related to fatigue stresses, interlayer strength, temperature stresses, and the strestrongdient of asphalt materials. Sangpetngam [10, 11] used the energy ratio theory as a basis for determining the direction of crack generation and crack expansion. The cracking mechanism of asphalt pavement surface cracks was analyzed by using ABAQUS finite element software to establish a three-dimensional model of asphalt pavement surface cracks [12–14], taking into account the stiffness gradient of the asphalt material, tire-pavement contact, and temperature stress. The method used in literature 14 et al. analyzed the cracking mechanism of asphalt pavements under static loads only by using ABAQUS finite element software, without considering the input of dynamic loads comprehensively. He Wei [15–17] Combining triaxial repeated load test, freeze-thaw splitting test, rupture test, etc. and finite element simulation, it was concluded that overloading is an important reason for the formation of surface cracks in asphalt pavement. In addition, many other studies have been conducted through experiments and field research [18] and established finite element simulations to discuss the influencing factors of asphalt pavement surface crack expansion respectively, and it is considered that the tensile stress caused by temperature drop is a very large influencing factor.

The formation of slip cracks often occurs first with interlayer slippage, followed by U-shaped cracking of the asphalt pavement surface layer due to excessive vehicle loading. This type of disease is more common in asphalt pavements and is usually divided into three stages, as shown in Figure 1, and has a greater impact. And mostly based on field sampling analysis as well as experimental methods. Bognacki et al. [19] sampled and analyzed
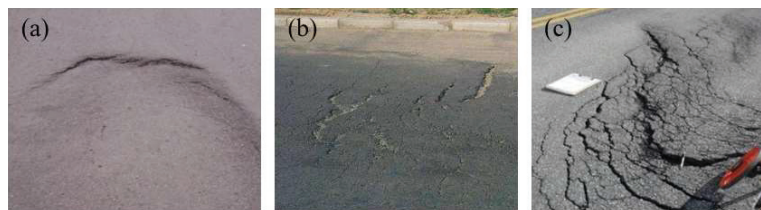

Figure 1   Slip cracks under mechanical action (a) Minor cases (b) Medium case (c) Severe cases.

the sections of airport roads where sliding occurred and studied the use of construction aggregates. Hachiya et al. [20] proposed methods and considerations for improving the interlayer strength by changing the interlayer bonding material [21]. The experimental analysis obtained that the inter-ply slip phenomenon occurs when the inter-ply shear stress of asphalt pavement under tire action is greater than its inter-ply shear strength, resulting in an inter-ply slip on the pavement surface and leading to slip cracks in the surface layer. Jon A. Epps et al. [22–25]. Summarized a large number of actual cases to conclude that the areas prone to slip cracking such as airports and highways often have large shear stresses, and pointed out that the main cause of slip cracking is the shear strength of the interlayer interface. There are also various simulation means or analysis methods on slip cracking studies, which effectively enhance computational efficiency [26–33].

The above studies have important implications [34–37]. But all of them have shortcomings in the research. On the one hand, the pavement slip cracking model considered in the above literature, using a quasi-dynamic model, does not take into account the combination of measured kinetic data with simulation and the secondary development of a joint kinetic model that is more consistent with the actual situation. On the other hand.

The contact relations between the surface layer-surface layer and surface layer-subgrade layer in previous studies are relatively set simple, mostly smooth or continuous, which differs greatly from the real asphalt pavement interlayer bonding situation. Therefore, in this study, based on a comprehensive study of a large number of domestic and international studies, a method based on the input of kinetic measured data, programming, and XFEM is proposed for the study of highway semi-rigid asphalt pavements. In addition, the cohesive zone intrinsic structure model is considered to develop a comprehensive study of asphalt pavement surface slip crack extension.

2 Mechanical Model

In this paper, a refined intrinsic structure model combining MATLAB secondary development and finite elements is established for the study of crack extensions on the surface layer of asphalt pavement as well as slip cracks for an engineering example of semi-rigid asphalt pavement on a highway. The implementation of extended finite elements in ABAQUS requires special settings in the interaction module, which requires selecting a specific region as the computational region of the XFEM and defining its material parameters appropriately. The MATLAB control program is run to define

the damage criterion for the material as well as the damage evolution law. In the subsequent study, simulations of the actual working conditions are performed by applying the corresponding parameters of the measured vehicle dynamics. Finally, the XFEM crack-related parameters are output in the output variables.

2.1 Mechanical Characterization and Evaluation of Cracks

For XFEM of semi-rigid asphalt pavement projects, the discontinuity function is chosen to be introduced to achieve a local approximation to the crack resolution theory. The unit decomposition is constructed using a K-order moving least squares approximation shape function, i.e.

$$u^h(x) = \sum_I \varphi_I^K(x) \cdot \left[u_I + \sum_{i=1}^m b_{iI} \cdot q_i(x) \right] \tag{1}$$

Where $q_i(x)$ – can be a monomial basis.

The displacement of any point within the cell $u(x)$ can be divided into a continuous part and a discontinuous part, i.e.

$$u = u_{cont} + u_{disc} \tag{2}$$

where u_{cont} is continuous in Ω, u_{disc} is discontinuous in Ω, and the discontinuity is at the crack surface.

A conventional finite element approximation is used to solve the continuous part of, i.e.

$$u_{cont} = \sum_{i \in N^s} N_i(x)u_i \tag{3}$$

where N^s – the set of all nodes in the discrete domain; N_i – the node shape function; u_i – the node displacement.

For the discontinuous part, it can be further divided into two cases, which are units without crack tips and with cracks completely cut, and units with crack tips that have not been completely cut. The discontinuous displacement of the former can be expressed as Equation (4), and the latter can be expressed as Equation (5).

$$u_{disc} = \sum_{i \in N^{cut}} \overline{N_i}(x)H(x)a_i \tag{4}$$

$$u_{disc} = \sum_{i \in N^{tip}} \overline{N_i}(x) \sum_j B_j(x)b_i^j \tag{5}$$

where,

> $H(x)$ – generalized Heaviside function (step function), equal to 1 on one side of the crack and -1 on the other side of the crack.
>
> N^{cut} – set of nodes where the support domain of the form function is completely cut by cracks.
>
> N^{tip} – the set of nodes where the support domain of the form function is partially cut by the crack, i.e. the set of nodes where the support domain of the form function contains the crack tip.
>
> a_i, b_i^j – node enhancement variables.

In this study, the maximum principal stress damage criterion is chosen for achieving the free expansion of cracks within the structure. One of the maximum principal stress damage criteria is as follows.

$$f = \left\{ \frac{\langle \sigma_{\max} \rangle}{\sigma_{\max}^0} \right\} \tag{6}$$

where, $\sigma_{\max}^0$ – the maximum allowable stress value, which can be considered as the tensile strength of the material.

> $\sigma_{\max}$ – Maximum principal stress.

In the calculations of this joint model, the activation or not of the XFEM cracking mechanism is determined by the following equation.

$$1.0 \le f \le 1.0 + f_t \tag{7}$$

where, f_t – the parameter used to adjust the incremental step to ensure that the damage criterion is met, is taken as 0.05.

2.2 Mechanical Testing of Interlayer Parameters of Asphalt Pavements

In this experimental study, we conducted interlaminar shear strength tests at different temperatures, using different amounts of adhesive layer materials, and under the action of different adhesive layer materials. A series of experiments were conducted to obtain data on the interlaminar properties under different conditions. A schematic diagram of the experimental model is shown in Figure 2. The model shows the ideal situation of interlaminar contact. We simulated the contact behavior between different layers in the actual asphalt pavement by placing an appropriate adhesive layer material in the model and applying shear forces.
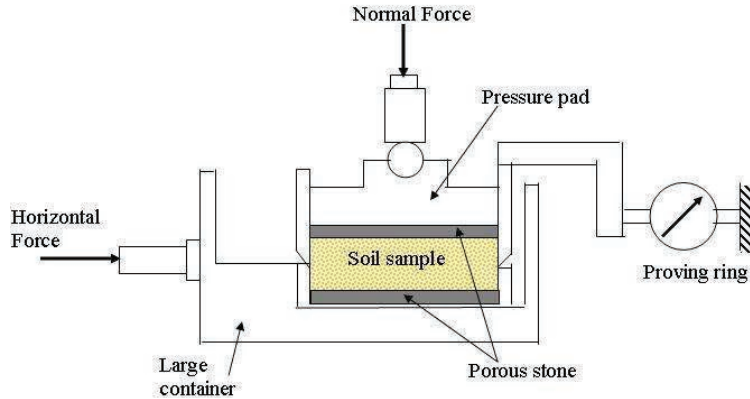
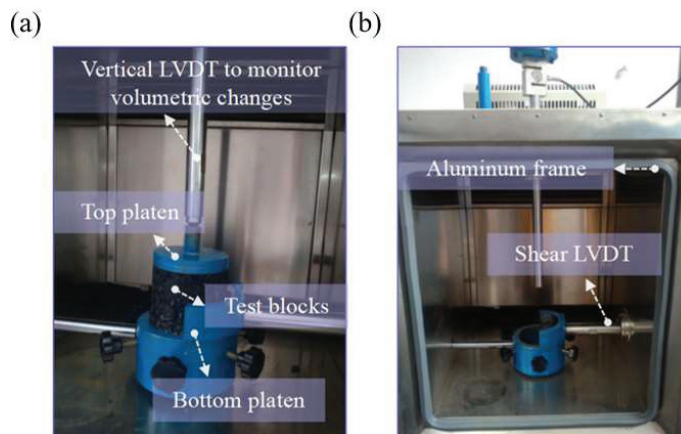**Figure 2** Schematic diagram of the ideal experimental model.

Figure 3 Straight shear test (a) Experimental test arrangement (b) Device appearance.

The arrangement of the specific experimental setup is shown in Figure 3. In the actual test, combined with the actual working conditions, the temperature was selected to test 60°C and 25°C, respectively. The sticky layer materials were emulsified asphalt and modified emulsified asphalt, and the sticky layer dosages were 0, 0.2, 0.4, and 0.6 kg/m^2. The experimental results are shown in Table 1. below, to obtain the shear strength parameters of various asphalt materials between layers required for the joint simulation. In addition, combined with the experimental results, it can be obtained that the selected range of interlayer strength for the upper layer-middle layer in this pavement crack cracking model is 0.1–0.5 MPa.

Table 1   Interlaminar strength test results

Bonding Layer Material Dosage/ (kg/m^2)	Material Type Temperature/°C	Emulsified Asphalt		Modified Emulsified Asphalt	
		Maximum Shear Force/N	Shear Strength/ MPa	Maximum Shear Force/N	Shear Strength/ MPa
0	25	4405	0.54	–	–
	60	472	0.06	–	–
0.2	25	4795	0.61	5150	0.656
	60	926	0.12	958	0.122
0.4	25	5474	0.697	5874	0.758
	60	880	0.112	1088	0.139
0.6	25	5298	0.675	6272	0.799
	60	812	0.103	1057	0.135

Table 2   Pavement structure and material parameters

Structural Layer	Materials	Thickness/cm	Modulus/MPa	Poisson's Ratio
Upper layer	AC-13	4	12900	0.25
Middle surface layer	AC-20	5	12500	0.35
lower layer	AC-25	6	14500	0.35
Grassroots	5% CTB	20	13500	0.25
Substrate	3% CTB	25	13000	0.25
Road base	Soil base	540	100	0.4

2.3 Kinetic Slip Cracking Model of XFEM

The road structure model is simplified into a multi-layer elastic system with an additional spring-damping effect, and the roadbed is an elastic half-space body. In addition, the computational cost of the refined model can be greatly improved by batching parameter input and optimal control of the Matlab program. As shown in Table 2.

In a practical implementation, the numerical simulation and analysis of cracks can be performed by modeling the crack geometry and inputting the corresponding boundary conditions and material parameters into the finite element software. The software will use the local approximation of crack resolution theory to calculate the stress and strain fields around the crack and further analyze the crack extension and effects. The kinetic theory analysis and finite element model are shown in Figure 4. When simulating the vehicle
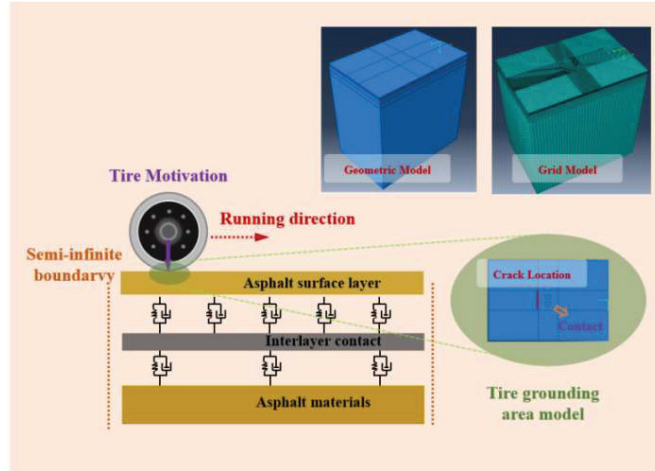
Figure 4   Joint finite element model under dynamic load.

Table 3   Wheel load and contact results of actual tests

Axial Load/kN	L*/m	0.6 L/m	d/m	Grounding Pressure/MPa
100	0.225	0.155	0.164	0.700
120	0.239	0.165	0.155	0.744
140	0.252	0.174	0.146	0.783
160	0.263	0.182	0.138	0.819
180	0.274	0.189	0.131	0.852
200	0.284	0.196	0.124	0.882

load in the area of action of the asphalt pavement, the reasonable study and description of the set parameters of the tire-pavement contact surface and the mechanical parameters is a very important step in the modeling.

Combined with the actual test results of wheel load contact with the ground, the tire grounding shape and grounding pressure were calculated for different axle load cases, and the results are shown in Table 3 below.

3 Surface Slip Cracking of Asphalt Pavement

During vehicle driving and braking, too low interlayer bond strength or insufficient surface material strength may produce interlayer slip in asphalt pavement and further lead to slip cracking. Through kinetic simulation, the asphalt surface layer slip crack formation level expansion law is studied.

3.1 Stress Field of Pavement Under Horizontal Load Before Slip

Extracting the stress field of the pavement under horizontal loading before the slip occurred. As shown in Figure 5, the transverse distribution of tensile stresses also shows that the tensile stresses behind the wheel tracks are at their peak, and the further away from the back of the wheel tracks the tensile stresses decrease sharply, even at the edge of the stress encryption zone the road surface is in a state of compression. The longitudinal tensile stress mainly acts in the upper layer and the middle layer is at the maximum value at the road surface, and gradually decreases from top to bottom before cracks appear, and the longitudinal tensile stress gradually tends to zero when the depth is located in the lower layer and below, that is, slip cracking often occurs only in the upper layer. Combined with the huge change in the value of tensile stress when the vehicle is braking, it can be considered likely that the asphalt pavement wheel track behind the higher longitudinal tensile stress produces open-type cracks along the direction of travel.

It can be seen that the shear stress on the pavement is mainly distributed on both sides of the wheel track, and combined with Figure 5(a), it can be seen that the shear stress on the pavement on both sides of the wheel track is in opposite directions, and its absolute maximum value appears on the outer side, while the shear stress on the pavement inside the wheel track is relatively small; as the transverse distance increases and reaches the outer side of the wheel track, the shear stress value reaches its peak and gradually decreases. In the depth direction, as shown in Figure 6, the maximum value of shear stress appears at the road surface, and mainly acts on the upper layer, almost 75% of the shear stress is concentrated in the upper layer, and the value of
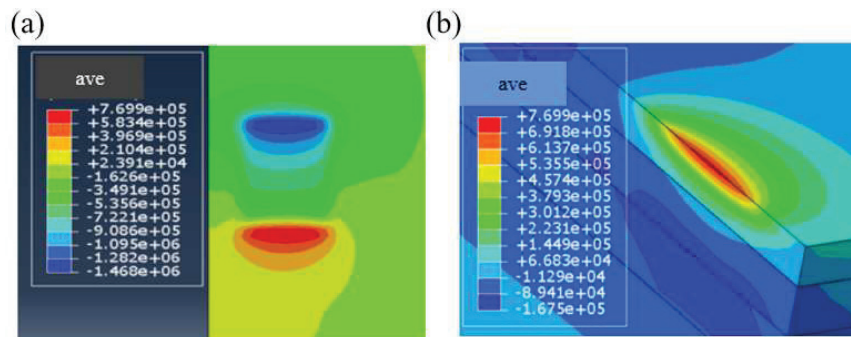

Figure 5 Longitudinal tensile stress cloud (a) Road surface cloud map (b) Cloud map of the depth along the road surface.
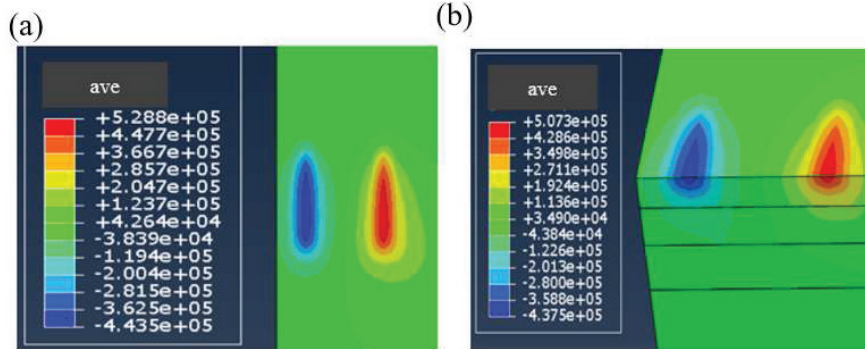
Figure 6   Shear stress cloud (a) Road surface cloud map (b) Depth cloud map along the road surface.

shear stress gradually decreases as it goes from top to bottom. In summary, it can be concluded that the larger shear stresses on both sides of the wheel track may lead to shear damage on both sides of the wheel track.

3.2 Pavement Structure Stress Field After the Initial Crack Generation

The process of asphalt pavement slip cracking is that the tensile stress in the direction of travel on the upper layer reaches the tensile strength of its material, producing an initial long crack in the transverse direction, followed by an oblique crack at approximately 45° to the initial crack due to the shear stress on both sides of the wheel track, and finally forming a U-shaped crack. In this section, the generation of its initial crack and the expansion after the generation of the initial crack will be studied. The initial crack can be seen as a 1.4 cm × 15 cm crack surface perpendicular to the pavement, and the crack starts from the surface of the upper layer, and crack does not penetrate the upper layer at this time. The longitudinal tensile stresses on the asphalt pavement after the introduction of the initial crack are shown in Figure 7(b). It can be seen that after the introduction of the initial crack, the stress along the depth direction at the crack in the surface layer of the asphalt pavement has reached the cracking stress strength, so the crack will penetrate the surface layer of the pavement; the longitudinal tensile stress at the middle surface layer directly below the initial crack has not reached the starting condition of cracking. Therefore, it can be assumed that after the cracking of the asphalt pavement surface layer, further expansion will be carried out only in the asphalt pavement surface layer.
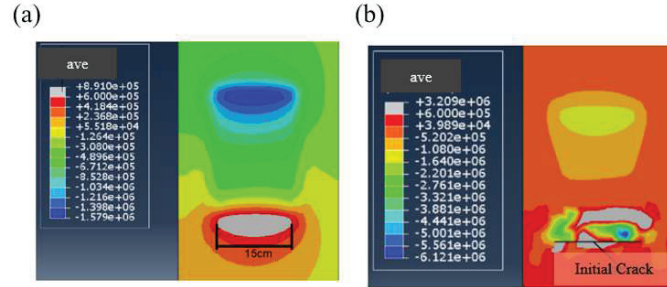
Figure 7   Crack initiation (a) Initial cracking (b) Longitudinal stress after crack development.
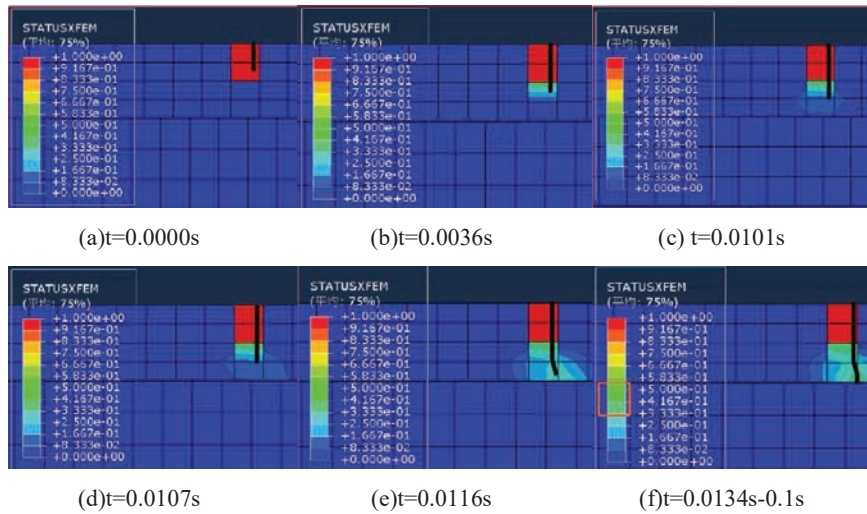

Figure 8   STATUSXFEM cloud at the crack.

3.3 Crack Extension Direction Study

The variation of STATUSXFEM at the midpoint of the precast crack at different times is shown in Figure 8, and the crack expansion path has been bolded. It can be seen from the figure that when the vehicle is braking, the instantaneous tensile stress on the road surface is huge, so much so that the tensile stress at the vertical crack tip of the crack reaches 0.6 MPa at 0.0036 s causing it to start expanding. The thinness of the upper layer caused the crack to have penetrated the upper layer at 0.0134 s. Because this is not only the midpoint of the precast crack, but also the maximum tensile stress, the vertical expansion rate here is the fastest and the shortest time, and the other locations

of the crack start to continue to expand laterally and U-shaped expansion in the direction of travel after 0.0134 s. Combined with Figure 8, it can be learned that the crack did not extend on the middle surface layer due to the presence of viscous layer oil to offset part of the stress transmission from top to bottom.

Where, when STATUSXFEM=0, the model crack has not reached the damage initiation criterion, then the crack has not expanded; when 0<STATUSXFEM<1, the model crack has met the damage initiation criterion, at this time the material began to accumulate damage, cracks began to appear, but did not appear macro cracking and expansion; when STATUSXFEM>1, the At this time, the damage accumulation has exceeded the critical value, the macroscopic crack formally opened and expanded.

4 Parametric Analysis of Surface Slip Cracking in Asphalt Pavements

The study of asphalt surface layer slip crack formation level expansion law is closely related to the main factors such as traffic load, surface layer thickness, interlayer shear strength, and surface layer material strength. Therefore, the influence of the above factors on the formation of slip cracks needs to be further analyzed.

4.1 Effect of the Interlayer Contact Form on Slip Cracking

The maximum longitudinal and maximum shear stresses on the upper layer of the pavement for different forms of interlayer contact can be obtained by varying the different layers, as shown in Figure 9.

When the interlayer is smooth, the maximum longitudinal tensile stress in the upper layer is 1.362 MPa, and when the interlayer is continuous, the maximum tensile stress in the upper layer is 0.7625 MPa, which is 44% less than that in the case of the smooth interlayer. When the interlayer is sprayed with viscous layer oil, the maximum tensile stress in the upper layer gradually decreases within a certain range as the interlayer strength gradually increases, and when the interlayer strength is 0.4 MPa afterwardards, the maximum tensile stress stops decreasing as the interlayer strength increases and stays at 0.769 MPa; when the interlayer is sprayed with viscous layer oil, the trend of the maximum tensile stress in the upper layer is the same as that of the sprayed viscous layer oil. When the interlayer strength increases gradually from 0.1 MPa to 0.3 MPa, the tensile stress decreases gradually, and when
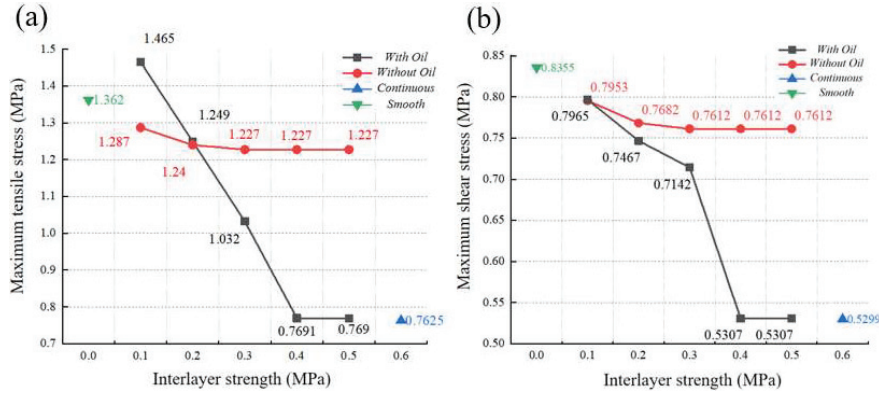
Figure 9 Maximum stress under different interlayer contacts (a) Longitudinal stress (b) Shear stress.

the interlayer strength is greater than 0.3 MPa, the maximum tensile stress in the upper layer is stabilized at 1.227 MPa. in addition, it can be seen from the figure that when the interlayer strength is 0.3 MPa and higher, the maximum tensile stress in the upper layer without spraying viscous layer oil between layers will be larger than that of the upper layer with spraying viscous layer oil by 37.3%, on the contrary, when the interlayer strength is low, the tensile stress on the upper layer without spraying sticky layer oil will be smaller. The maximum shear stress on the road surface is 0.8355 MPa when the interlayer is smooth, and the minimum is 0.5299 MPa when the interlayer is continuous, which is 36.6% lower than the former. In the case of the same interlayer strength, after the interlayer strength is greater than 0.1 MPa, the shear stress suffered by the pavement surface in the case without sticky layer oil is greater than that in the case with sticky layer oil. Within a certain range, the shear stress on the pavement surface decreases gradually with the increase of interlayer strength, but it is stable after the interlayer strength is 0.3 MPa, which is 0.7612 MPa without sticky layer oil and 0.5307 MPa with sticky layer oil, which is 30.3% smaller than the former.

The extracted interlaminar forces for different forms of interlaminar contact are shown in Figure 10, where the stiffness degradation rate CSDMG of interlaminar adhesion is observed for the case with sticky layer oil, and the interlaminar contact force CSHEAR2 in the travel direction is used for the case without sticky layer oil.

It can be seen that when the interlayer strength in the case of unsprayed viscous layer oil is 0.3 MPa, the maximum shear stress suffered by the layer is
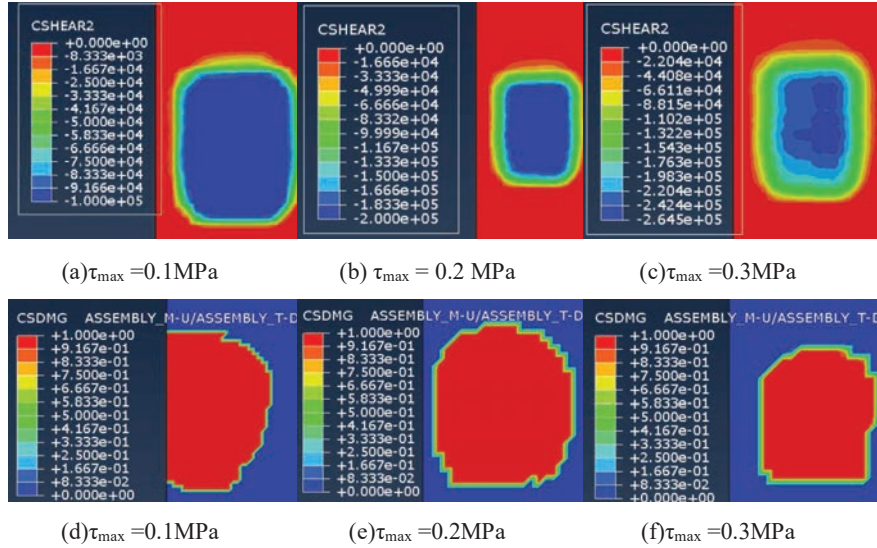
(a)τ_{max} =0.1MPa   (b) τ_{max} = 0.2 MPa   (c)τ_{max} =0.3MPa

(d)τ_{max} =0.1MPa   (e)τ_{max} =0.2MPa   (f)τ_{max} =0.3MPa

Figure 10   Interlayer forces for different contact forms.

(a)τ_{max} =0.1MPa   (b) τ_{max} = 0.2 MPa   (c)τ_{max} =0.3MPa

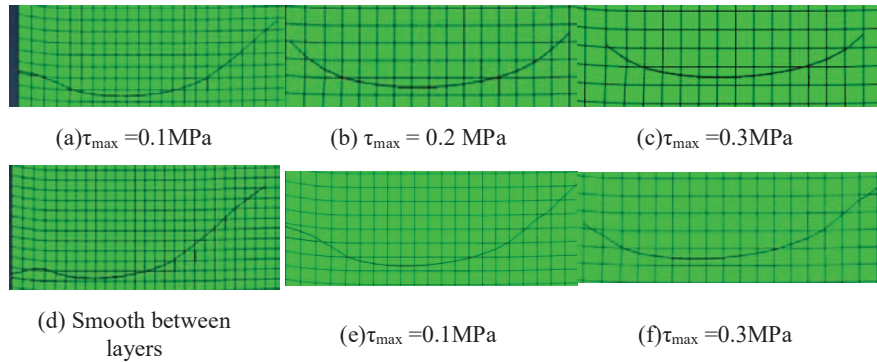(d) Smooth between layers   (e)τ_{max} =0.1MPa   (f)τ_{max} =0.3MPa

Figure 11   Crack extension diagram.

0.2645 MPa, and with the increase of interlayer strength this interlayer shear stress also no longer changes; with the interlayer strength of viscous layer oil is 0.4 MPa, the interlayer does not occur viscous failure and slip, which will not be discussed in this section.

The calculation results of the crack extension part are shown in Figure 11. In the figure, (a) (b) (c) is with sprayed viscous layer oil, and (d) (e) (f) is for sprayed viscous layer oil. It can be seen that the length of the crack is gradually shortened as the interlayer viscous strength is larger when the other

conditions are the same with spraying sticky layer oil. And no slip cracking occurs when the interlayer strength is greater than 0.4 MPa; when it is sprayed with viscous layer oil, the crack length is longer and the crack opening angle is larger compared with the interlayer viscous condition, and the crack length reaches the maximum when the interlayer is smooth.

Combined with the above research results, it can be seen that the interlayer spraying of viscous layer oil will greatly reduce the size of the force on the upper layer of the pavement, and reduce the size of its force area; as the interlayer strength gradually increases, the probability of interlayer slippage will gradually decrease, and the area of interlayer slippage will also gradually decrease. Therefore, we can conclude that we should choose to use interlayer viscous oil in actual construction, choose suitable viscous oil material according to the cost and construction requirements and conditions, and appropriately increase the viscous oil spraying to ensure that the interlayer strength reaches the requirements as much as possible.

4.2 Effect of Axial Load on Slip-cracking Stress

The distribution of longitudinal tensile stresses along the center line of the wheel track in the direction of traffic under different axle loads is shown in Figure 12. It can be seen that as the axle load gradually increases, the transverse tensile area of the pavement gradually increases, and the total tensile area also gradually increases; the change law of stress distribution before and after the slip is the same as the distribution law of tensile stress
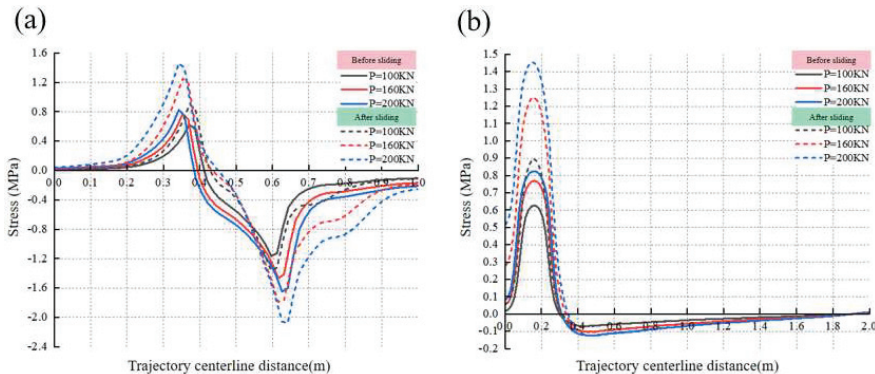

Figure 12   Comparison of wheel track stress before and after a slip (a) Before and afterslip comparison (b) Before and afterslip comparison.

(a)P=100kN   (b)P=120kN   (c)P=140kN

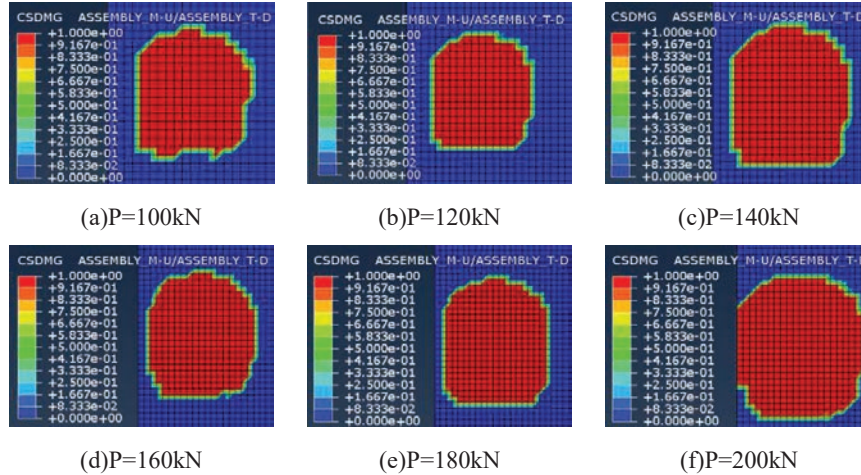(d)P=160kN   (e)P=180kN   (f)P=200kN

Figure 13   Schematic diagram of interlayer adhesion failure.

in the direction of traffic, and the longitudinal tensile stress of the pavement after the slip under the same axle load is greater, and the tensile area is wider, and the peak position is unchanged.

In addition, the failure diagram of interlaminar adhesion damage under the action of different axle loads is shown in Figure 13. It can be seen that as the vehicle axle load increases, the failure area of interlaminar adhesion gradually increases; the vehicle axle load has a very strong influence on the force between the layers, and the increase of axle load will increase the probability of slip lesions between the layers.

4.3 Influence of Surface Elastic Modulus on Interlaminar Forces

The maximum interlaminar shear stresses between the upper-middle pavement layers under different elastic modulus conditions before the interlaminar slip was generated are shown in Figure 14. As the elastic modulus of the upper layer increases, the interlaminar shear stress gradually decreases, but the decreasing trend is gradually leveling off, and the elastic modulus is 6.1% less at 14500 MPa than at 7500 MPa. The different surface elastic moduli (7500, 1150 and 14500) were chosen for the analysis in order to investigate the effect of surface elastic modulus on interlaminar forces and to explore its effect on the variation of the system properties. This choice was considered based on covering the different material properties and the available experimental data support.
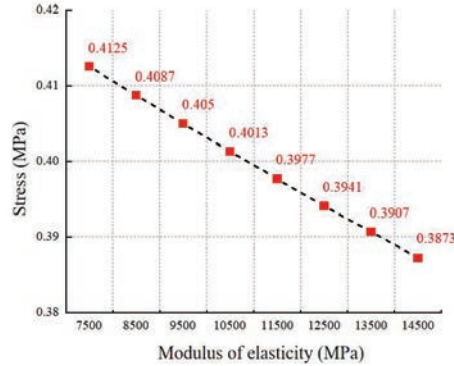
Figure 14   Interlaminar shear stress with different elastic modulus.

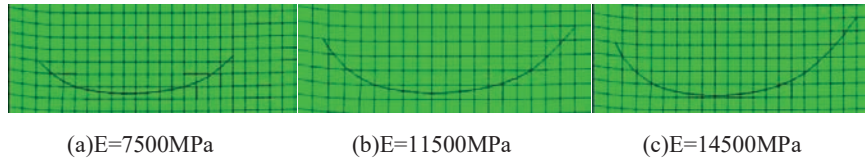(a)E=7500MPa   (b)E=11500MPa   (c)E=14500MPa

Figure 15   Schematic diagram of crack extension.

After the simulation calculation, it can be learned that with the gradual increase of the elastic modulus of the upper layer, the damage failure area of the interlaminar adhesion is gradually reduced, but the reduction is not very obvious, and here the cases of elastic modulus of 7500 MPa, 11500 MPa, and 14500 MPa are selected to talk about, and the schematic diagram of the interlaminar bond failure is shown in Figure 15. It can be seen that as the modulus of elasticity of the upper layer gradually increases, the adhesive contact failure area between the layers gradually decreases, the main failure area is directly below the front of the wheel track, and the bond failure situation directly below the rear of the wheel track gradually gets better. This indicates that the probability of interlaminar slip generation gradually decreases as the modulus of elasticity of the upper layer increases, but the decrease is not obvious under the other conditions that remain unchanged.

In addition, a comparison of the crack expansion of the pavement with slip cracking for the cases of upper layer modulus of elasticity of 7500 MPa, 11500 MPa, and 14500 MPa respectively is shown in Figure 14. It can be seen that, when other conditions do not change, as the modulus of elasticity of the upper layer material gradually increases, the crack expansion appears as follows: (1) the crack length gradually increases; (2) the U-shaped opening

of the crack becomes smaller, i.e., the deflection angle of the crack expansion becomes larger; (3) the growth of the inner crack length is smaller than that of the outer one.

Combined with the above research results, it can be found that increasing the elastic modulus of pavement surface layer material will lead to the increase of both longitudinal tensile and shear stresses on the surface layer of the pavement structure, which will increase the probability of pavement cracking; on the other hand, the interlayer force on the layers will have a certain decrease, which will reduce the probability of interlayer slippage and damage. Considering the force situation of the pavement structure, the elastic modulus of the pavement surface layer material selected above 12500 MPa is more suitable.

5 Study on the Correlation Degree of Influencing Factors Based on Grey Correlation Theory

Gray correlation analysis is the use of gray correlation order [34] to characterize the strength, magnitude, and order of the relationships between factors, which can be used to determine the degree of influence between system factors or the degree of influence of factors on the main behavior of the system. In this section, gray correlation theory will be used to investigate the degree of influence of each influencing factor on several major stress components that lead to pavement slip cracking.calculated as shown in Equation (8).

$$\Delta_{ij} = |Y_{i0} - Y_{ij}| \tag{8}$$

The gray correlation coefficient r_{ij} is calculated as shown in Equation (9).

$$r_{ij} = \frac{\Delta_{\min} + \rho\Delta_{\max}}{\Delta_{ij} + \rho\Delta_{\max}} \tag{9}$$

where $\Delta_{\min}$ denote the minimum and maximum values of all absolute differences. Δ_{ij} respectively. ρ – Resolution factor $0 < \rho < 1$ generally takes the value of.

The gray correlations of each stress component of interlayer strength, axial load, and elastic modulus of the upper layer were calculated separately and summarized as shown in Table 4. For the longitudinal tensile stress, which is the main cause of tension cracks at the bottom of U-shaped slip cracking in asphalt pavement, the degree of influence of each influencing factor is axial load > interlayer strength > modulus of elasticity of the upper

Table 4   Gray correlation of different influencing factors

	Longitudinal Tensile Stress (MPa)	Shear Stress (MPa)	Interlayer Shear Stress (MPa)
Interlayer strength	0.6671	0.6630	–
Axle load	0.7805	0.7268	0.5537
Modulus of elasticity	0.5728	0.5737	0.5833

layer; for the shear stress, which is the main cause of shear cracks on both sides of U-shaped slip cracking in asphalt pavement, the degree of influence of each influencing factor is: axial load > interlayer strength > modulus of elasticity of the upper layer For the main cause of interlayer shear stress of interlayer slip damage, the degree of influence of each influencing factor is the interlayer modulus of elasticity > axial load.

6 Conclusion and Discussion

(1) Interlayer bonding damage leads to separate stress on the surface layer of asphalt pavement; the longitudinal tensile stress behind the wheel track leads to cracking at the bottom of the U-shaped crack; under the action of shear stress, both sides of the wheel track deflect toward the direction of crack expansion, forming U-shaped cracks.

(2) After the interlayer strength is 0.3 MPa, the interlayer bonding damage is no longer deteriorated; the use of interlayer cohesive layer oil and increasing interlayer strength can improve the damage of asphalt pavement surface slip cracks.

(3) When the vehicle axle load increased from 100 kN to 200 kN, the maximum longitudinal tensile stress of asphalt pavement surface layer increased by 62.6%, the maximum shear stress increased by 57.3%, and the maximum interlayer shear stress increased by 21.1%, and the interlayer bond damage area also gradually increased, and the length of the final slip crack gradually increased.

(4) In the process of increasing the modulus of elasticity of asphalt pavement surface layer from 7500 MPa to 14500 MPa, the maximum longitudinal tensile stress of asphalt pavement surface layer increased by 10.2%, the maximum shear stress increased by 18.3%, but the maximum interlayer shear stress decreased by 6.1%, the area of interlayer adhesion damage gradually decreased, and the length of the final slip crack increased and the U-shaped opening became smaller.

References

[1] Ministry of Transport of the People's Republic of China. People's Daily [EB/OL].

[2] Wang Shuangxi. Analysis of asphalt concrete pavement diseases and countermeasures. Heilongjiang Transportation Science and Technology, 2011, 34(11): 29–36.

[3] Zhao Shuming, Liu Yajuan. Analysis of the causes of asphalt pavement damage on highways. Highway Traffic Technology (Applied Technology Edition), 2013, 9(07): 24–5+63.

[4] Weng Meize, Wang Huoming, Feng Yong. Current status and development of asphalt pavement maintenance technology. China Water Transport (Academic Edition), 2007, (02): 59–60.

[5] Zhang HW, Wang XY, Liu ZZ, et al. Analysis of shear stresses in intersection pavements under moving non-uniform loads. Journal of Chang'an University (Natural Science Edition), 2016, 36(06): 26–31+47.

[6] Mao Cheng. Research on crack formation mechanism and expansion behavior of asphalt pavement. Southwest Jiaotong University, 2004.

[7] Chen Yuanzhao. Research on the Prevention and Control Technology of Asphalt Pavement Diseases on Long Longitudinal Slopes. Chang'an University, 2011.

[8] Dinegdae Y H, Birgisson B R. Effects of truck traffic on top-down fatigue cracking performance of flexible pavements using a new mechanics-based analysis framework. Road Materials & Pavement Design, 2016: 1–19.

[9] Emery J. Evaluation and Mitigation of Asphalt Surface Course Top-Down Cracking, F, 2005.

[10] Sangpetngam B, Birgisson B, Roque R. Development of Efficient Crack Growth Simulator Based on Hot-Mix Asphalt Fracture Mechanics. Transportation Research Record Journal of the Transportation Research Board, 2003, 1832: 105–112.

[11] Zhang Shanshan. Study on cracking mechanism of Top-Down cracks in asphalt pavement. Chang'an University, 2012.

[12] Yi Xin. Three-dimensional finite element method to analyze the top-down crack expansion of asphalt pavemen. Hunan University, 2006.

[13] Hu Yuan. Mechanism of Top-Down Crack Formation in Asphalt Pavements. Huazhong University of Science and Technology, 2012.

[14] He Wei. Analysis of the causes and influencing factors of Top-Down cracks in asphalt pavements in semi-arid areas. Hebei University, 2021.

[15] Lv Guangyin. Research on Top-Down cracking mechanism of flexible base asphalt pavement. Chang'an University, 2008.

[16] Yang SQ, Liao SY, Guo M, et al. Study of factors influencing Top-down cracking in asphalt pavements based on thermal coupling. Highway Engineering: 1–12.

[17] Niu Liqiang. Analysis of the causes of Top-Down cracks in asphalt pavements. Road Construction Machinery and Construction Mechanization, 2017, 34(01): 69–72.

[18] Li F, Sun LJ. Finite element analysis of the causes of Top-Down cracking in asphalt pavements. Road Traffic Technology, 2006, (06): 1–4.

[19] Bognacki C J, Frisvold A, Bennett T. Investigation of Asphalt Pavement Slippage Failures on Runway 4R-22L, Newark International Airport. 2007.

[20] Kai S U, Sun L, Hachiya Y, et al. Analysis of shear stress in asphalt pavements under actual measured tire-pavement contact pressure. 2008.

[21] Button J W. Asphalt Overlays with Mlraflb Fabric – The Slippage Question – On Airport Pavements. 2018.

[22] Chen D-H. Slippage Failure of a New Hot-Mix Asphalt Overlay. Journal of Performance of Constructed Facilities, 2010, 24(3).

[23] Yang K, Li R, Yu Y, et al. Evaluation of interlayer stability in asphalt pavements based on shear fatigue property. Construction and Building Materials, 2020, 258.

[24] Joli, P., Azouz, N., Wezdou, M.B. and Neji, J. 2023. Nonlinear Analysis of Cable Structures with Geometric Constraints. European Journal of Computational Mechanics. 31, 04 (Feb. 2023), 433–458.

[25] Rezaiee-Pajand, M. and Karimipour, A. 2019. Stress Analysis by Two Cuboid Isoparametric Elements. European Journal of Computational Mechanics. 28, 5 (Dec. 2019), 373–410.

[26] Yaacob H, Hainin M R, Rasid A, et al. Information for the Malaysian Asphalt Industry towards better pavement interlayer bonding. Sains Malaysiana, 2014, 43(3): 467–474.

[27] Canestrari F, Santagata E. Temperature effects on the shear behavior of tack coat emulsions used in flexible pavements. International Journal of Pavement Engineering, 2005, 6(1): 39–46.

[28] Eedula S R. Tackcoat acceptance criterion. Dissertations & Theses – Gradworks, 2007.

[29] Park K. Potential-based fracture mechanics using cohesive zone and virtual internal bond modeling. Dissertations & Theses – Gradworks, 2009.

[30] Kim Y R. Cohesive zone model to predict fracture in bituminous materials and asphaltic pavements: a state-of-the-art review. International Journal of Pavement Engineering, 2011.

[31] Yuan Xinzhe. Numerical simulation study of long-life micro overlay interlayer durability of asphalt pavement. Beijing Jiaotong University, 2017.

[32] Vo T P, Guan Z W, Cantwell W J, et al. Low-impulse blast behavior of fiber-metal laminates. Composite Structures, 2011, 94(3).

[33] Phadnis V A, Makhdum F, Roy A, et al. Drilling in carbon/epoxy composites: Experimental investigations and finite element implementation. Composites Part A, 2013, 47.

[34] Canestrari F, Ferrotti G, Partl M N, et al. Advanced testing and characterization of interlayer shear resistance. Bituminous Paving Mixtures 2005. 2005: 69–78.

[35] SONG S H. Fracture of asphalt concrete: A cohesive zone modeling approach considering viscoelastic effects. University of Illinois at Urbana- Champaign. 2006.

[36] Luo Qingcheng, Xu Guoxin. Gray correlation analysis with applications. Gray correlation analysis with applications, 1989.

[37] Phadnis V A, Makhdum F, Roy A, et al. Drilling in carbon/epoxy composites: Experimental investigations and finite element implementation [J]. Composites Part A, 2013, 47.

Biography

Yin Zhenyu received the bachelor's degree in Hydrogeology and Engineering Geology from Jiaozuo Institute of Technology (now known as Henan

Polytechnic University) in 2001, the master's degree in Geological Engineering from Henan Polytechnic University in 2008. He is currently working as a lecturer at the School of Civil and Transportation Engineering of Henan University of Urban Construction. His research areas and directions include pavement engineering and geotechnical engineering.